

## Research Paper

# Implementation of Fuzzy PID Controller in Cascade with Anti-Windup to Real-Scale Test Equipment for Pavements

Oscar Javier REYES-ORTIZ, Juan Sebastián USECHE-CASTELBLANCO\*  
German Leandro VARGAS-FONSECA

*Faculty of Engineering*  
*Universidad Militar Nueva Granada*

Bogota, Colombia

e-mail: {oscar.reyes, german.vargas}@unimilitar.edu.co

\*Corresponding Author e-mail: u1801739@unimilitar.edu.co

In the industry and academia, large-scale equipment has been developed, which requires control systems that provide safety and efficiency with the lowest possible energy consumption. In the industrial cascade control system, nested controllers have been a versatile tool for the control of large-scale equipment. Research shows that these types of controllers improve their performance with the integration of artificial intelligence algorithms and prevention methods against controller saturation. For this reason, this paper presents the development of a fuzzy proportional-integral-derivative (PID) controller in cascade with anti-windup (AW) for full-scale test equipment for pavements. In this study, the mathematical expressions for the equipment, the design of the controller and additional systems for comparison, simulation and analysis are developed. The main objective is to test the functionality of this type of nested controllers for these systems.

**Key words:** pavements; cascade control; fuzzy; anti-windup.

## 1. INTRODUCTION

Big industrial processes and heavy machinery developed for the productive and academic sector require systems that guarantee high efficiency with the least use of resources and the smallest environmental impact [1]. The development of a robust infrastructure for academic research has been accomplished in the recent years for the study of pavements. Large-scale tests have become more frequent because they simulate the behaviour of the road with real loads and operating conditions [2]. However, these control tests and the equipment used consume large amounts of energy, and their control is affected by exterior dis-

turbances. In addition, their mathematical representations are of higher- order or non-linear [3].

Recently, cascade control has been used for this kind of processes. Nested control allows reducing the order of the control loops and decreases the effects of secondary variable disturbances on the primary variable [4]. This is done with multiple control loops which stabilize the states that directly affect the central variable [5].

On the other hand, controllers based on fuzzy logic are an alternative to deal with the nonlinearities in large-scale systems [6]. This is because fuzzy logic controllers work with open systems that are designed according to the behaviour of the process and not with a mathematical description [7].

Some works are presented below with relation to fuzzy cascade control. In [8], the development of a fuzzy cascade controller for the transport of crude oil in a pipeline using a PLC-based controller is presented. In the same work, it is concluded that this type of controllers reduces the overshoot of the system. The authors of [9] developed an industrial evaporator using a hybrid PID and fuzzy PID cascade system. They demonstrated how the fuzzy controller helps with the control of the nonlinearities of the system. Another implementation of cascade control systems is presented in [10]. Here, the main objective is to control part of the system of an electric vehicle. Additionally, artificial intelligence techniques are implemented for the optimization of parameters of the PID controllers. The performance of the frequency response obtained is better than when using the traditional structure.

This work presents the design of a fuzzy PID controller in cascade to which an AW security system is added. This control is applied to the large-scale equipment used for the study of pavements. In the following sections, the mathematical description of the process, the implementation of the PID control system, cascade PID, and cascade fuzzy PID are presented. This is done in order to compare the operation of the main controller with the others. Then, the adaptation of the AW system to the fuzzy controller is carried out. Finally, the responses of the setup obtained by simulation are analysed using the different controllers and the AW system. The study is concluded with the section about the efficiency of this type of controllers.

## 2. MATERIALS AND METHODS

### 2.1. Load application system

The load application system shown in Fig. 1 is a testing set developed by the geotechnical research group from the Nueva Granada Military University [11].



FIG. 1. Large-scale test equipment.

The physical parameters for the solution of the mathematical representation of the system were obtained with the help of this equipment.

The equipment's operation is carried out by using a hydraulic system that produces a maximum force of 80 000 N. This force is transmitted to the pavement through a system that simulates a truck. The load to the structure of the road is generated using a hydraulic circuit presented in Fig. 2.

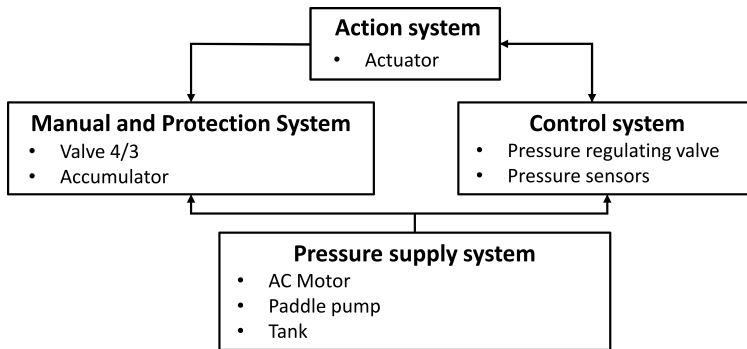


FIG. 2. Hydraulic system.

The operation of the system starts with a variable vane pump, which generates a constant flow rate of 0.36 l/s. The pressure is regulated with a proportional relief valve with an analogue input voltage of  $\pm 10$  V. The actuator is a hydraulic cylinder that is coupled to the equipment rolling system. Addition-

ally, there is a valve for manual control and an accumulator to avoid overpressure peaks caused by the response between the tires and the pavement. The control system is feedback controlled by pressure sensors at different points.

The mathematical representation of the system is obtained by assuming some performance characteristics as shown in [12] where a constant flow rate pump is assumed in time, not taking into account the Coulomb friction, and assuming the oil as an incompressible fluid.

The sum of the forces that are present in the hydraulic actuator is shown in Eq. (2.1):

$$(2.1) \quad pA_2 - p_cA_1 = M\ddot{x} + B_c\dot{x} + k_ex,$$

where  $p$  and  $p_c$  are the pressures of the chambers cylinder. The input pressure  $p$  is the control variable.  $A_1$  and  $A_2$  are the small and large cross-sectional areas of the actuator,  $x$  is the displacement of the cylinder,  $M$  is the mass of the rod-piston assembly,  $B_c$  is the viscous resistance coefficient,  $k_e$  is the rigidity of the coupling between the cylinder and the tires, and  $p_c$  is the outlet pressure to the tank and it is considered equal to 0.

The valve output flow is the variable that controls the system. This flow responds proportionally to the spool displacement ( $y$ ). In Eq. (2.2), the analysis of the forces resulting from the valve is obtained:

$$(2.2) \quad (k_vv - p)A = m\ddot{y} + B_s\dot{y} + k_sy,$$

where  $k_v$  is the pressure gain constant,  $v$  is the set point of pressure in voltage,  $A$  is the area of the spool cross-section,  $m$  is the spool mass.  $B_s$  is the viscosity coefficient, and  $k_s$  represents the stiffness of the spool spring.

Equation (2.3) expresses the flow to the hydraulic actuator.  $K_Q$  is the flow constant,  $K_l$  the leakage constant,  $V_b$  is the entry chamber volume, and  $\beta_e$  is the oil bulk modulus

$$(2.3) \quad Q_E = K_Qx - K_l p - \frac{V_b}{\beta_e} \dot{p}.$$

The inflow  $Q_E$  is equal to  $Q_B - Q_S$ .  $Q_B$  is the pump flow that for this case is assumed constant and  $Q_S$  is the output flow through the proportional relief valve. The proportional valve is described by the linear function of the following equation:

$$(2.4) \quad Q_S = k_qy + k_{c1}p,$$

where  $k_q$  is the constant that relates the displacement of the spool with the opening hole and  $k_{c1}$  is the discharge coefficient by pressure.

Table 1 shows the values of the system parameters obtained from the real equipment.

**Table 1.** Model parameters.

Parameter	Description	Value
$M$	Rod-piston mass	1.63 kg
$m$	Spool mass	0.33 kg
$K_Q$	Flow constant	$3.72\text{e-}3 \text{ m}^2/\text{s}$
$K_l$	Leakage constant	$8.3\text{e}3 \text{ m}^3/(\text{MPa} \cdot \text{s})$
$V_b$	Volume of the entry chamber	$2.13\text{e-}3 \text{ m}^3$
$\beta_e$	Fluid bulk module	1.2e3 MPa
$k_e$	Rigidity of the cylinder coupling	9.74e2 N/m
$A_2$	Large cross-section area of the piston	$1.56\text{e-}3 \text{ m}^2$
$B_c$	Viscous resistance coefficient	$0.45 \text{ N} \cdot \text{s}/\text{m}$
$k_q$	Spool – opening hole relation	$0.0697 \text{ m}^2/\text{s}$
$k_{c1}$	Coefficient of discharge by pressure	$8.05\text{e-}9 \text{ m}^3/(\text{Pa} \cdot \text{s})$
$A$	Cross-section area spool	$3.12\text{e-}5 \text{ m}^2$
$B_s$	Spool viscosity coefficient	$0.38 \text{ N} \cdot \text{s}/\text{m}$
$k_s$	Rigidity of the spool spring	3.7e2 N/m
$k_v$	Voltage-pressure gain	1.4e6 Pa/V

Figure 3 shows the response of the testing system to a step input as a set point. A stable behaviour is confirmed with error in a steady state of position and time of establishment around 12 seconds.

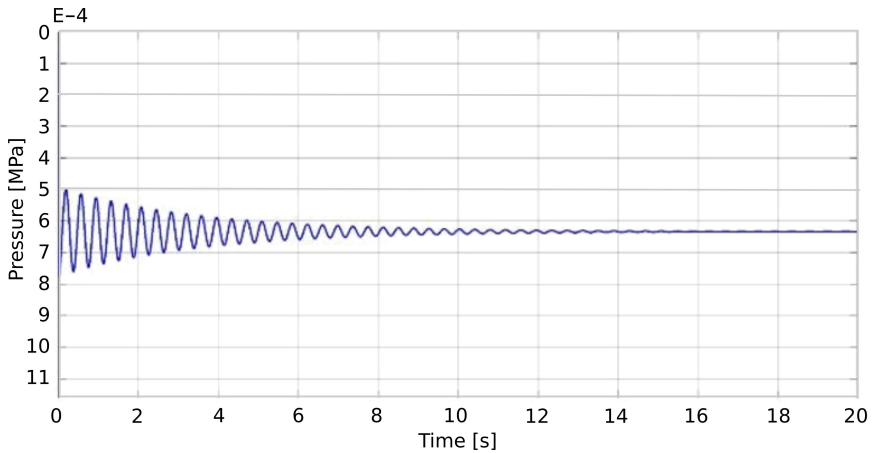


FIG. 3. Open loop.

Organizing the system into equations of state is obtained:

$$\begin{aligned}
 \dot{x} &= v_x, \\
 \dot{v}_x &= -\frac{k_e}{M}x - \frac{B_c}{M}v_x + \frac{A_2}{M}p, \\
 \dot{y} &= v_y, \\
 \dot{v}_y &= -\frac{k_s}{m}y - \frac{B_s}{m}v_y - \frac{A}{m}p + \frac{Ak_v}{m}v, \\
 \dot{p} &= \frac{K_Q\beta_e}{V_b}x + \frac{\beta_e k_q}{V_b}y + \frac{\beta_e(k_{c1} - K_l)}{V_b}p - \frac{\beta_e Q_B}{V_b}.
 \end{aligned}
 \tag{2.5}$$

## 2.2. Test controllers

To study the behaviour of the fuzzy controller, a traditional PID and a PID in the cascade are implemented to the system.

The PID controller is calculated by obtaining the system transfer function in Laplace domain. As a result, a fifth-order system is obtained with a PIDD2D3. For the solution, the desired polynomial of robustness is calculated with Eq. (2.6). This is done to decrease the sensitivity of the system against disturbances

$$\begin{aligned}
 B_d(s) &= (s^2 + 2\rho w_n s + w_n^2)^2(s + \alpha), \\
 w_n &= \frac{4.6}{\rho t_s},
 \end{aligned}
 \tag{2.6}$$

where  $\rho$  is the damping constant of the system,  $t_s$  is the plant establishment time in the open loop, and  $\alpha$  is the non-dominant pole of the system defined as  $5w_n$ .

For the cascaded PID controller, the control loop is defined as shown in Fig. 4.

As it is observed, the fifth-order is conserved and it is uncoupled in two nested controllers: one secondary and one primary. The first is a PI that controls the position of the spool and serves as a slave control of a PID that controls the system pressure.

The constants of the controllers with the segmented system are calculated. For the PID controller, the third-order set is used, which relates the pressure to the movement of the hydraulic actuator. The position model of the valve spool is used for the PI. The fact that the stabilization time of the slave must be faster than the master must be taken into account.

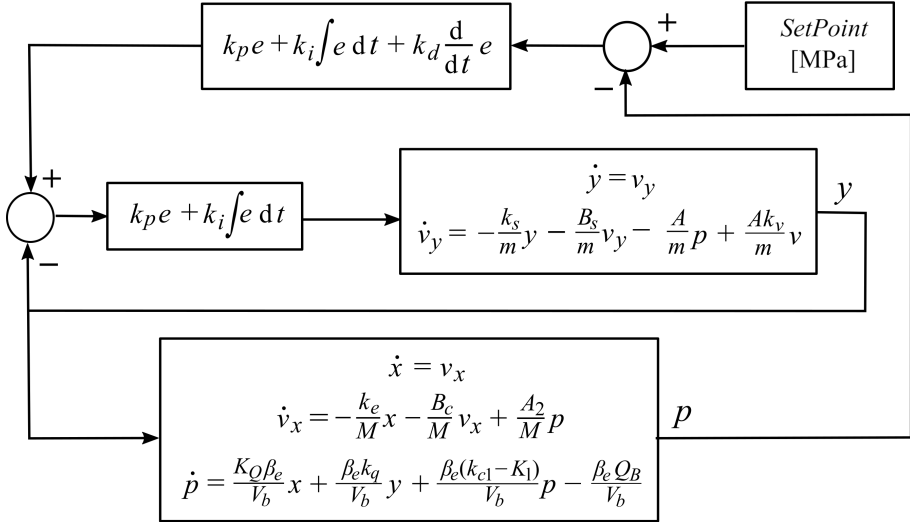


FIG. 4. Cascade control.

2.3. Fuzzy controller in cascade

The general control scheme is the same as in Fig. 4, with the only difference that in the two control loops, a fuzzy PD is developed. The integral constant is not linked to the fuzzy controller to ensure the steady-state position error equal to zero. The modified control scheme is presented in Fig. 5.

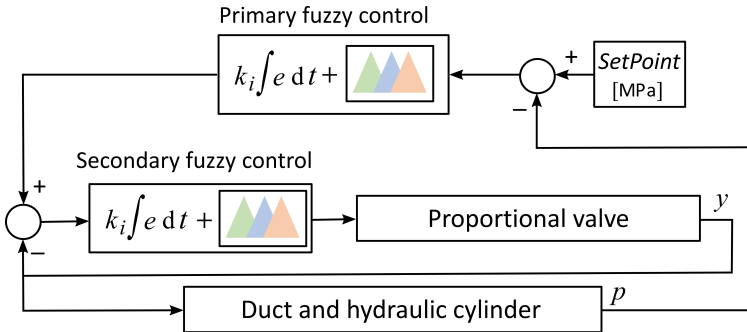


FIG. 5. Fuzzy cascade control.

The two fuzzy controllers for the system are based on the membership functions and the linguistic logic of [13]. Membership functions can take values between 0 and 1.

The controller begins with the fuzzification that represents giving fuzzy or linguistic values assigned by a degree of belonging. to the real values [14]. To

obtain the degree of belonging of each value, Eqs (2.7) and (2.8) are applied representing a trapezoidal and triangular function, respectively

$$(2.7) \quad \mu(x) = \begin{cases} \frac{x-a}{b-a} & \text{for } a < x < b, \\ 1 & \text{for } b < x < c, \\ \frac{d-x}{d-c} & \text{for } c < x < d, \\ 0 & x < a \text{ or } x > d, \end{cases}$$

$$(2.8) \quad \mu(x) = \begin{cases} \frac{x-a}{b-a} & \text{for } a < x < b, \\ 1 & \text{for } x = b, \\ \frac{c-x}{c-b} & \text{for } b < x < c, \\ 0 & x < a \text{ or } x > c. \end{cases}$$

For the fuzzification, three belonging functions are proposed for each entry (positive, negative, and medium). The union of these three functions is known as a fuzzy set [15]. Each fuzzy system is designed with two input sets – one for the error and another one for its derivative. The working ranges of each fuzzy set are established based on the possible error behaviour. Figure 6 illustrates the

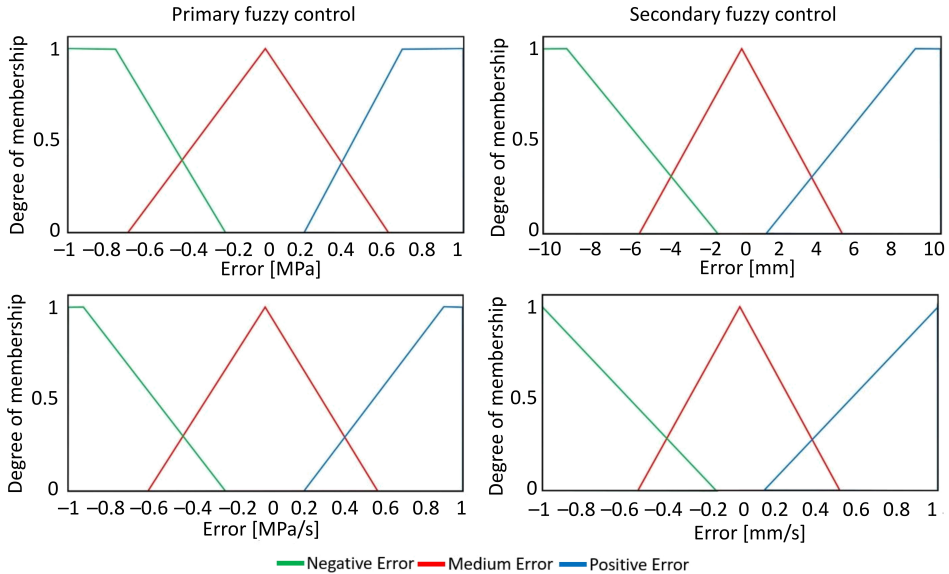


FIG. 6. Fuzzy input sets.

different fuzzification functions for both controllers. In this case, each fuzzy set is symmetrically centred at zero.

For the output, a fuzzy set is also parameterized. The output interval depends on the working ranges of the actuator that will execute the action. For the study case, the control depends on the variation of the relief valve of  $\pm 10 v$  and the spool of  $\pm 10 \text{ mm}$ . In Fig. 7, the parameterization of the outputs can be observed.

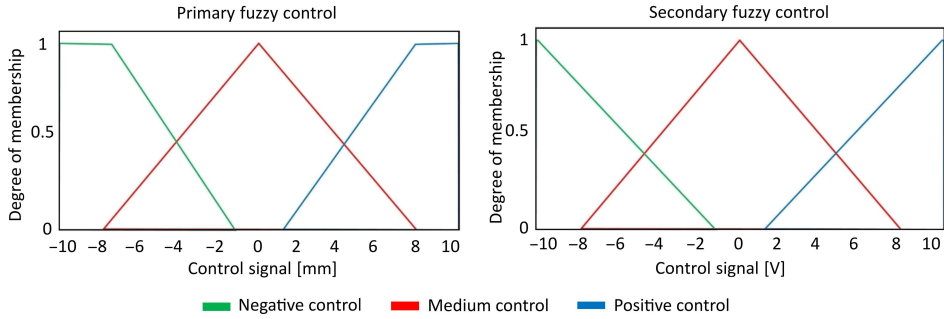


FIG. 7. Fuzzy output sets.

The Mamdani method with type rules (if-else) [16] is used to relate the input and output sets. The rules for the two systems are presented in Table 2. In this case, these are equal since the error presents the same behaviour, and the same action is required for the two controllers.

**Table 2.** System rules.

Error	Speed error	Control
Negative error	Negative error	Negative
Negative error	Medium error	Negative
Negative error	Positive error	Negative
Medium error	Negative error	Medium
Medium error	Medium error	Medium
Medium error	Positive error	Medium
Positive error	Negative error	Positive
Positive error	Medium error	Positive
Positive error	Positive error	Positive

The system has nine rules that relate the different input and output functions. From the previous table, it is observed that the system responds directly to the input error. The error derivative serves to attenuate the control signal when it is in a contrary direction.

The centroid method presented in [17] is used for the defuzzification. Its equation is as follows:

$$(2.9) \quad y_{\text{centroid}} = \frac{\sum_{x=X}^R x \mu_A(x)}{\sum_{x=X}^R \mu_A(x)},$$

where  $R$  is the number of rules,  $X$  is the max value, and  $\mu_A(x)$  is the value of belonging. This process is applied to the fuzzy sets shown in Fig. 7 and through this, the control signal is obtained.

#### 2.4. Anti-windup implementation

The AW model is implemented with the system presented in [18]. The method consists of creating a feedback on the difference between the control signal and the effective output to the system. This allows the indefinite integration of the control to be null while the system is in saturation. This provides better stability to the system and it creates an effective recovery of the integral variables when it is working at the limits [19]. Figure 8 shows the model implemented on an integral variable in a PID control.

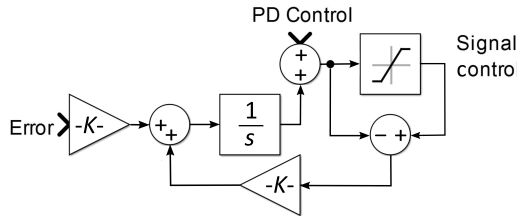


FIG. 8. Anti-windup architecture for the integral variable.

$K$  of the error ( $K_e$ ) according to the theory must be greater than  $K$  from the difference in the saturator ( $K_s$ ). For determining the impact of the anti-windup constants values, three different cases shown in Eq. (2.10) are taken. The value of  $K_e$  for all cases will be equal to  $K_i$  calculated for the previous loops

$$(2.10) \quad \begin{aligned} \text{case 1 : } & K_s = K_e, \\ \text{case 2 : } & K_s = 1.2K_e, \\ \text{case 3 : } & K_s = 0.8K_e. \end{aligned}$$

3. ANALYSIS AND RESULTS

Figure 9 depicts the different control loops for the system. A traditional PID system, a PID in cascade and a fuzzy PID in cascade are presented. For the controls, the differential equations using blocks are implemented.

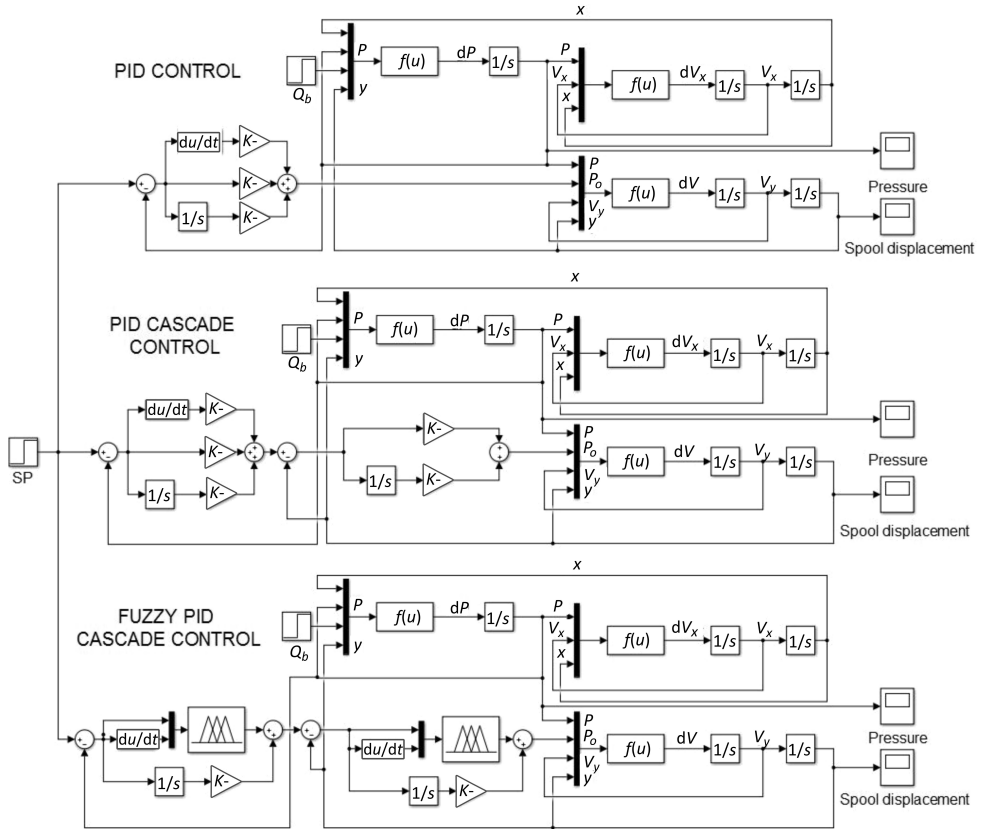


FIG. 9. Control systems.

Figure 10 shows the controllers response to an input of the blocks. The figure shows the differences in the type of response, the PID and PID cascade have a critically damped response form. For its part, the fuzzy system is a linguistic and not precise, and its response has a minimum overshoot.

The three controllers satisfy the stabilization time within a tolerance interval. It is observed that the PID in cascade responds faster than the other two. The fuzzy controller has a special feature: its response form denotes a smooth behaviour similar to tracking systems.

Figure 11 shows that the control signal of the systems maintains the same behaviour as the response.

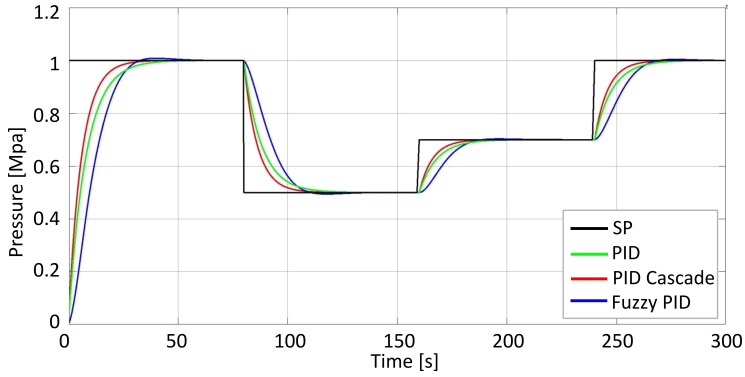


FIG. 10. System response.

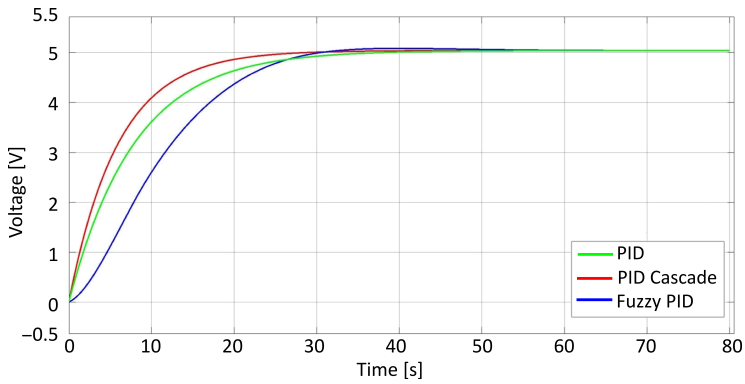


FIG. 11. Control signals.

In Figs 12 and 13, the system receives two different pressure disturbances. The first is a possible bump on the track and the second noise is the acquisition

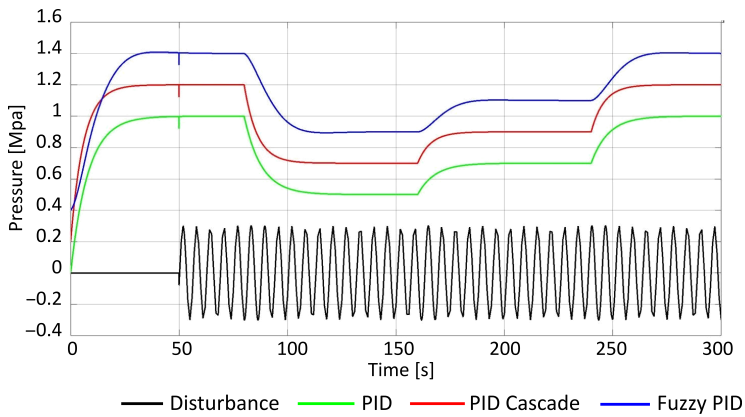


FIG. 12. Harmonic disturbance.

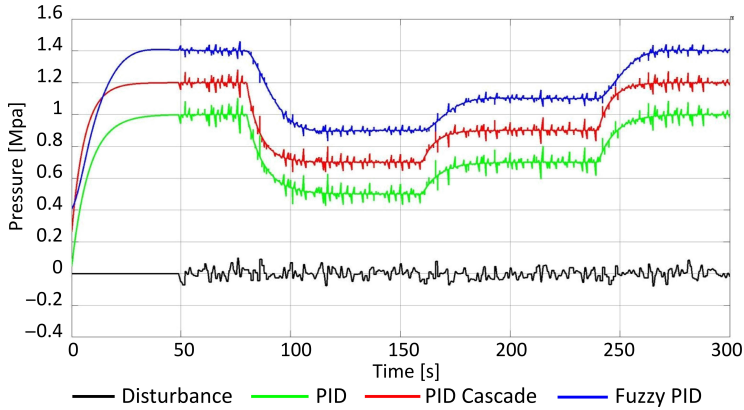


FIG. 13. Random disturbance.

of the sensor signal. An offset is added to the answers to separate and observe them better.

From the previous images, it is observed how the three controllers respond in a similar way against harmonic disturbances, suppressing them totally. This may be because their desired polynomials were designed in robustness mode.

For the second case in random perturbations, it is observed how the fuzzy system suppresses and diminishes some peaks. This is because the controller within its flexibility attenuates disturbances. This behaviour is typical for the tracking systems that are smooth at first and acts as a regulator for impulse disturbances.

It is expected that in a real implementation, its behaviour against system disturbances will be improved compared to traditional controllers. This is because, as mentioned above, its control is designed based on system behaviour and not a mathematical description.

Figure 14 shows the scheme of the diffuse system with the implementation of the AW model for the integrators.

Figure 15 shows the response without and with AW for the three cases of Eq. (2.10). It is observed that the coupled model does not interfere with normal setup response within the working range of the actuators in either case.

For observing the AW function, a sinusoidal signal is applied that saturates the system. The response is presented in Fig. 16 where it is observed that there is a displacement between the reference signal and the testing setup. This is normal in tracking systems or smooth start. The behaviour shows that these systems regulate the continuous integration of the controller when it is saturated.

As shown in Fig. 16, the plant with AW responds normally when the setpoint re-enters the operating ranges. The above is observed in Fig. 17. On the other

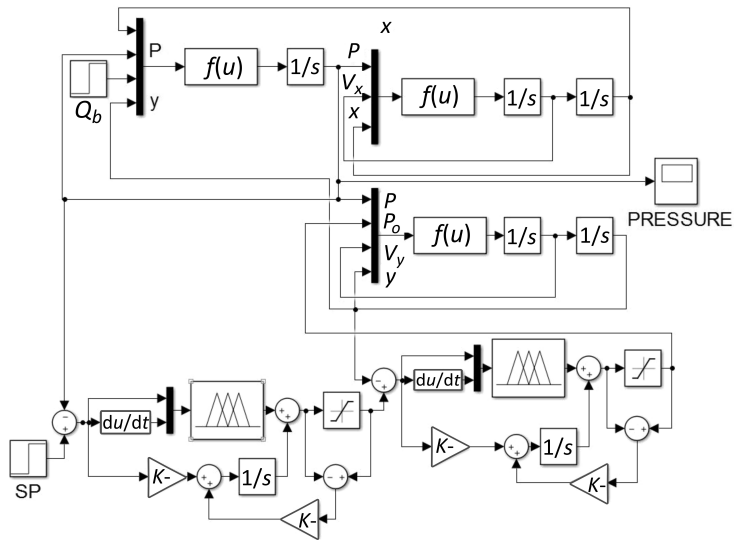


FIG. 14. Anti-windup fuzzy system.

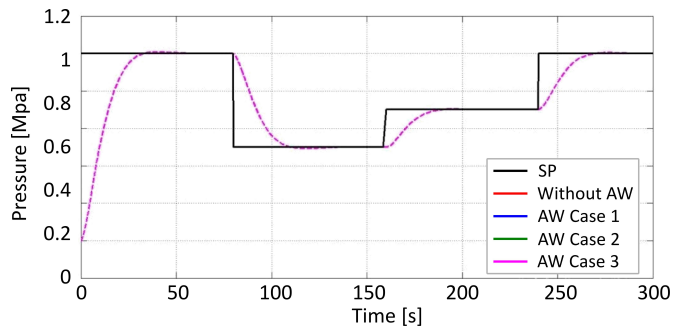


FIG. 15. Response within the operating range.

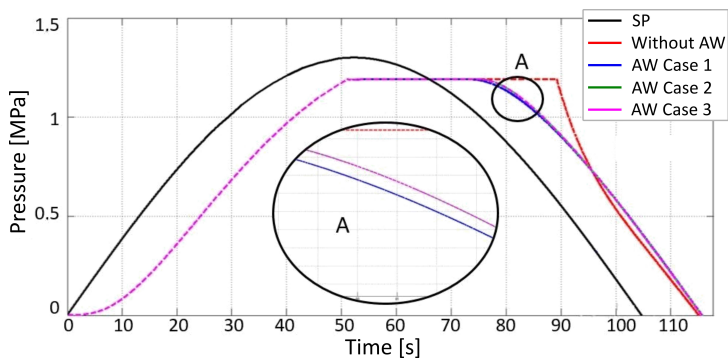


FIG. 16. The response outside the operating range.

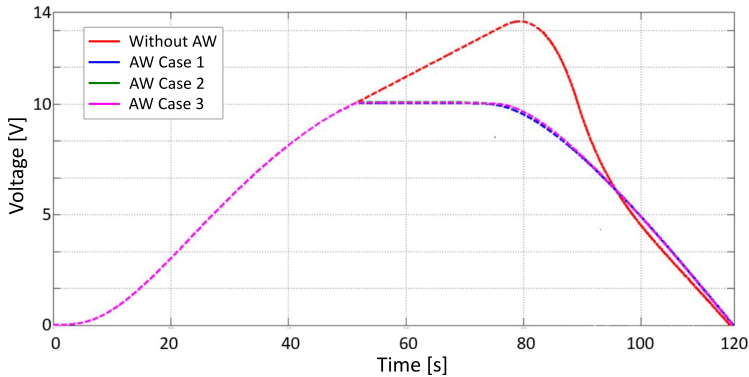


FIG. 17. Control signal before saturator.

hand, it is also observed that for case 1 of Eq. (2.3), the AW system has a higher response speed than in the other two cases.

Figure 17 shows how the control signal of the system without Anti-Windup before the saturator, continues to integrate the error signal in time even if the system is at its operating limit.

#### 4. CONCLUSIONS

This work demonstrates the effectiveness and robustness of the implementation of a diffuse cascade controller with AW for a large-scale test equipment for pavements. The implementation of such type of controlling system is a viable alternative to traditional controllers.

Fuzzy logic controllers have a better behaviour against disturbances than traditional controllers do because this kind of controllers uses a response of follow-up control.

The decoupling control cascade provides a better design by reducing the order of the system and control variables that have a direct impact on the principal signal. A disadvantage of these systems is an increase of the computational cost by using several controllers and the need to measure the feedback variables.

The AW systems allow adding a safety factor inside the system. This controls the continuous integration of the controller's error even in a saturated state.

#### ACKNOWLEDGEMENTS

This research was conducted under the IMP-ING-2931 high-impact project funded by the Vice-Rector of Research at Universidad Militar Nueva Granada. The authors acknowledge and thank for this support.

## REFERENCES

1. YANG W., LI L., Efficiency evaluation of industrial waste gas control in China: A study based on data envelopment analysis (DEA) model, *Journal of Cleaner Production*, **179**: 1–11, 2018.
2. DU PLESSIS L., ULLOA-CALDERON A., HARVEY J.T., COETZEE N.F., Accelerated pavement testing efforts using the Heavy Vehicle Simulator, *International Journal of Pavement Research and Technology*, **11**(4): 327–338, 2018.
3. WERSÄLL C., NORDFELT I., LARSSON S., Resonant roller compaction of gravel in full-scale tests, *Transportation Geotechnics*, **14**: 93–97, 2018.
4. ILLIĆ B., MILOŠ M., ISAKOVIĆ J., Cascade nonlinear feedforward-feedback control of stagnation pressure in a supersonic blowdown wind tunnel, *Measurement*, **95**: 424–438, 2017.
5. JIA B., MIKALSEN R., SMALLBONE A., ZUO Z., FENG H., ROSKILLY A.P., Piston motion control of a free-piston engine generator: A new approach using cascade control, *Applied Energy*, **179**: 1166–1175, 2016.
6. CHANG W.-J., QIAO H.-Y., KU C.-C., Sliding mode fuzzy control for nonlinear stochastic systems subject to pole assignment and variance constraint, *Information Science*, **432**: 133–145, 2018.
7. NAGHIBI S.R., PIRMOHAMADI A.A., MOOSAVIAN S.A.A., Fuzzy MTEJ controller with integrator for control of underactuated manipulators, *Robotics and Computer-Integrated Manufacturing*, **48**: 93–101, 2017.
8. PRIYANKA E.B., MAHESWARI C., THANGAVEL S., Online monitoring and control of flow rate in oil pipelines transportation system by using PLC based Fuzzy-PID controller, *Flow Measurement and Instrumentation*, **62**: 144–151, 2018.
9. VERMA O.P., MANIK G., JAIN V.K., Simulation and control of a complex nonlinear dynamic behavior of multi-stage evaporator using PID and Fuzzy-PID controllers, *Journal of Computational Science*, **25**: 238–251, 2018.
10. PADHY S., PANDA S., MAHAPATRA S., A modified GWO technique based cascade PI-PD controller for AGC of power systems in presence of plug in electric vehicles, *International Journal of Engineering, Science and Technology*, **20**(2): 427–442, 2017.
11. CAMACHO-TAUTA J., REYES-ORTIZ O., DA FONSECA A.V., RIOS S., CRUZ N., RODRIGUES C., Full-scale evaluation in a fatigue track of a base course treated with geopolymers, *Procedia Engineering*, **143**: 18–25, 2016.
12. ACUÑA-BRAVO W., CANUTO E., AGOSTANI M., BONADEI M., Proportional electro-hydraulic valves: An Embedded Model Control solution, *Control Engineering Practice*, **62**: 22–35, 2017.
13. CHEN J., ZHU H., ZHANG L., SUN Y., Research on fuzzy control of path tracking for underwater vehicle based on genetic algorithm optimization, *Ocean Engineering*, **156**: 217–223, 2018.
14. WANG Y., JIN Q., ZHANG R., Improved fuzzy PID controller design using predictive functional control structure, *ISA Transactions*, **71**: 354–363, 2017.
15. KARAKOSE M., YETIS H., AKIN E., Sine-square embedded fuzzy sets versus type-2 fuzzy sets, *Advanced Engineering Informatics*, **36**: 43–54, 2018.

16. ASADI M., Optimized Mamdani fuzzy models for predicting the strength of intact rocks and anisotropic rock masses, *Journal of Rock Mechanics and Geotechnical Engineering*, **8**(2): 218–224, 2016.
17. CASTILLO O., AMADOR-ANGULO L., CASTRO J.R., GARCIA-VALDEZ M., A comparative study of type-1 fuzzy logic systems, interval type-2 fuzzy logic systems and generalized type-2 fuzzy logic systems in control problems, *Information Science*, **354**: 257–274, 2016.
18. ADEGBEBE A. A., HEATH W.P., A framework for multivariable algebraic loops in linear anti-windup implementations, *Automatica*, **83**: 81–90, 2017.
19. TURNER M.C., KERR M., A nonlinear modification for improving dynamic anti-windup compensation, *European Journal of Control*, **41**: 44–52, 2018.

*Received June 7, 2019; accepted version August 7, 2019.*

---

*Published on Creative Common licence CC BY-SA 4.0*

